

# Supramolecular Microcontact Printing and Dip-Pen Nanolithography on Molecular Printboards

Christiaan M. Bruinink,<sup>[a]</sup> Christian A. Nijhuis,<sup>[a]</sup> Mária Péter,<sup>[a]</sup> Barbara Dordi,<sup>[b]</sup> Olga Crespo-Biel,<sup>[a]</sup> Tommaso Auletta,<sup>[a]</sup> Alart Mulder,<sup>[a]</sup> Holger Schönherr,<sup>[b]</sup> G. Julius Vancso,<sup>[b]</sup> Jurriaan Huskens,<sup>\*,[a]</sup> and David N. Reinhoudt<sup>\*,[a]</sup>

**Abstract:** The transfer of functional molecules onto self-assembled monolayers (SAMs) by means of soft and scanning-probe lithographic techniques—microcontact printing ( $\mu$ CP) and dip-pen nanolithography (DPN), respectively—and the stability of the molecular patterns during competitive rinsing conditions were examined. A series of guests with different valencies were transferred onto  $\beta$ -cyclodextrin ( $\beta$ -CD-) terminated SAMs and onto reference hydroxy-terminated SAMs.

Although physical contact was sufficient to generate patterns on both types of SAMs, only molecular patterns of multivalent guests transferred onto the  $\beta$ -CD SAMs were stable under the rinsing conditions that caused the removal of the same guests from the reference SAMs. The formation of kineti-

cally stable molecular patterns by supramolecular DPN with a lateral resolution of 60 nm exemplifies the use of  $\beta$ -CD-terminated SAMs as molecular printboards for the selective immobilization of printboard-compatible guests on the nanometer scale through the use of specific, multivalent supramolecular interactions. Electroless deposition of copper on the printboard was shown to occur selectively on the areas patterned with dendrimer-stabilized gold nanoparticles.

**Keywords:** cyclodextrins • host-guest systems • lithography • molecular printboards • multivalency

## Introduction

The ability to transfer functional molecules onto surfaces on the nanometer scale is one of the enabling principles in the field of nanotechnology. Generally, there are two strategies for the transfer of molecules onto surfaces: 1) the use of templates (for example, patterns of self-assembled monolayers (SAMs) or polymers) to direct and control the selective deposition of molecules from solution; 2) active deposition onto surfaces by means of a patterning element (for exam-

ple, a stamp or a probe). The advantage of the latter patterning strategy is that the transfer of molecules onto surfaces does not rely on expensive photolithographic procedures and does not require processing conditions that are incompatible with several interesting types of functional molecules (for example, biomolecules) or susceptible to cross-contamination by nonspecific binding. Therefore, direct-patterning strategies in the micro- and nanometer regime, such as soft lithography<sup>[1,2]</sup> and scanning-probe lithography (SPL),<sup>[3]</sup> are extensively used for immobilizing functional molecules on surfaces. Examples include microcontact printing ( $\mu$ CP)<sup>[1]</sup> of proteins on glass<sup>[4]</sup> or of polymers on reactive SAMs on gold<sup>[5]</sup> and dip-pen nanolithography (DPN)<sup>[6,7]</sup> of DNA on gold and glass.<sup>[8]</sup> However, in most cases, the immobilization of molecules on the surface is accomplished either by covalent binding to the surface, or to SAMs consisting of anchoring molecules, or by nonspecific physisorption.

For some years our group has been exploiting *supramolecular* interactions, which combine the advantages of chemisorption and physisorption, to immobilize functional molecules on surfaces. Supramolecular interactions are directional and specific and allow fine-tuning of the adsorption/desorption processes at receptor surfaces,<sup>[9]</sup> which is not feasible for conventional routes of immobilizing molecules on

[a] C. M. Bruinink, C. A. Nijhuis, Dr. M. Péter, O. Crespo-Biel, Dr. T. Auletta, Dr. A. Mulder, Dr. J. Huskens, Prof. Dr. D. N. Reinhoudt  
Supramolecular Chemistry and Technology  
MESA<sup>+</sup> Institute for Nanotechnology, University of Twente  
P.O. Box 217, 7500 AE Enschede (The Netherlands)  
Fax: (+31) 53-489-4645  
E-mail: j.huskens@utwente.nl  
d.n.reinhoudt@utwente.nl

[b] Dr. B. Dordi, Dr. H. Schönherr, Prof. Dr. G. J. Vancso  
Materials Science and Technology of Polymers  
MESA<sup>+</sup> Institute for Nanotechnology, University of Twente  
P.O. Box 217, 7500 AE Enschede (The Netherlands)

Supporting Information for this article is available on the WWW under <http://www.chemeurj.org/> or from the author.

surfaces. Cyclodextrins (CDs) and their derivatives are attractive receptor molecules for application in receptor surfaces, as these molecules have been known to accommodate and form inclusion complexes with various organic guest molecules in aqueous solutions through hydrophobic interactions.<sup>[10,11]</sup>  $\beta$ -CD adsorbates containing multiple attachment points form SAMs on gold with a high degree of order, in which the recognition sites are pointing toward the outer interface of the monolayer in a quasihexagonal lattice.<sup>[12,13]</sup> This high degree of order and dense packing of the monolayer are prerequisites for the application of these SAMs in sensor applications in general,<sup>[14]</sup> and specifically in our  $\beta$ -CD SAMs.<sup>[9]</sup> These conditions render the (hydrophobic) recognition sites of all  $\beta$ -CD receptors on the surface essentially identical for guest complexation and minimize nonspecific adsorption.

The interaction strength of small, monovalent guest molecules to these  $\beta$ -CD SAMs has been studied by electrochemical impedance spectroscopy (EIS)<sup>[13]</sup> and surface plasmon resonance (SPR)<sup>[15]</sup> spectroscopy. Such guest molecules bind to  $\beta$ -CD SAMs with a binding strength that is identical to the intrinsic interaction strength with native  $\beta$ -CD in solution. Application of guest molecules that can form *multivalent* interactions offers a tool to fine-tune the overall interaction strength from reversible to permanent binding to the surface. This central property is exploited in the use of  $\beta$ -CD SAMs as molecular printboards<sup>[16]</sup> onto which it is possible to position multivalent guests. For this purpose, a divalent printboard-compatible guest molecule<sup>[17]</sup> has been specifically designed to study multivalent interactions at the printboard.<sup>[18,19]</sup> The contrasting binding behavior of this molecule and, in general, multivalent molecules compared to monovalent guest molecules is that the former molecules are capable of forming additional interactions and, therefore, have higher overall binding strengths with the  $\beta$ -CD surface. The overall interaction strength of the divalent guest molecule to the  $\beta$ -CD SAM was five orders of magnitude higher than the binding strength of any monovalent guest molecule. Our group has also reported the use of multivalent guests such as dendrimers<sup>[9]</sup> and polymers<sup>[20]</sup> that exhibit even stronger interactions with  $\beta$ -CD SAMs. The advantage of dendrimers is that the number of interactions with the printboard can be easily tuned by adjusting the dendrimer generation.<sup>[21]</sup>

The successful positioning of functional printboard-compatible guest molecules into molecular patterns on surfaces by supramolecular  $\mu$ CP and supramolecular DPN was reported previously.<sup>[22]</sup> The reversibility of supramolecular binding allows, in principle, the preparation of stable molecular patterns (for example, by printing or writing) under one set of conditions and erasure of these patterns under other conditions.

Herein, we present the first systematic study that addresses the stability of molecular patterns on the printboard towards rinsing conditions in relation to the number of binding functionalities (that is, valency). Transfer by supramolecular  $\mu$ CP of a series of different guest molecules, with 1–

64 binding functionalities per molecule, onto the printboard and onto a reference SAM, as well as the stability of the patterns upon rinsing, was examined by friction-force atomic force microscopy (AFM). Supramolecular DPN was carried out to investigate the potential of this serial technique for writing local, high-stability molecular patterns with lateral dimensions of less than 100 nm on the printboard. Finally, electroless deposition of copper was exploited to extend the application of molecular printboards to the fabrication of metal patterns.

## Results and Discussion

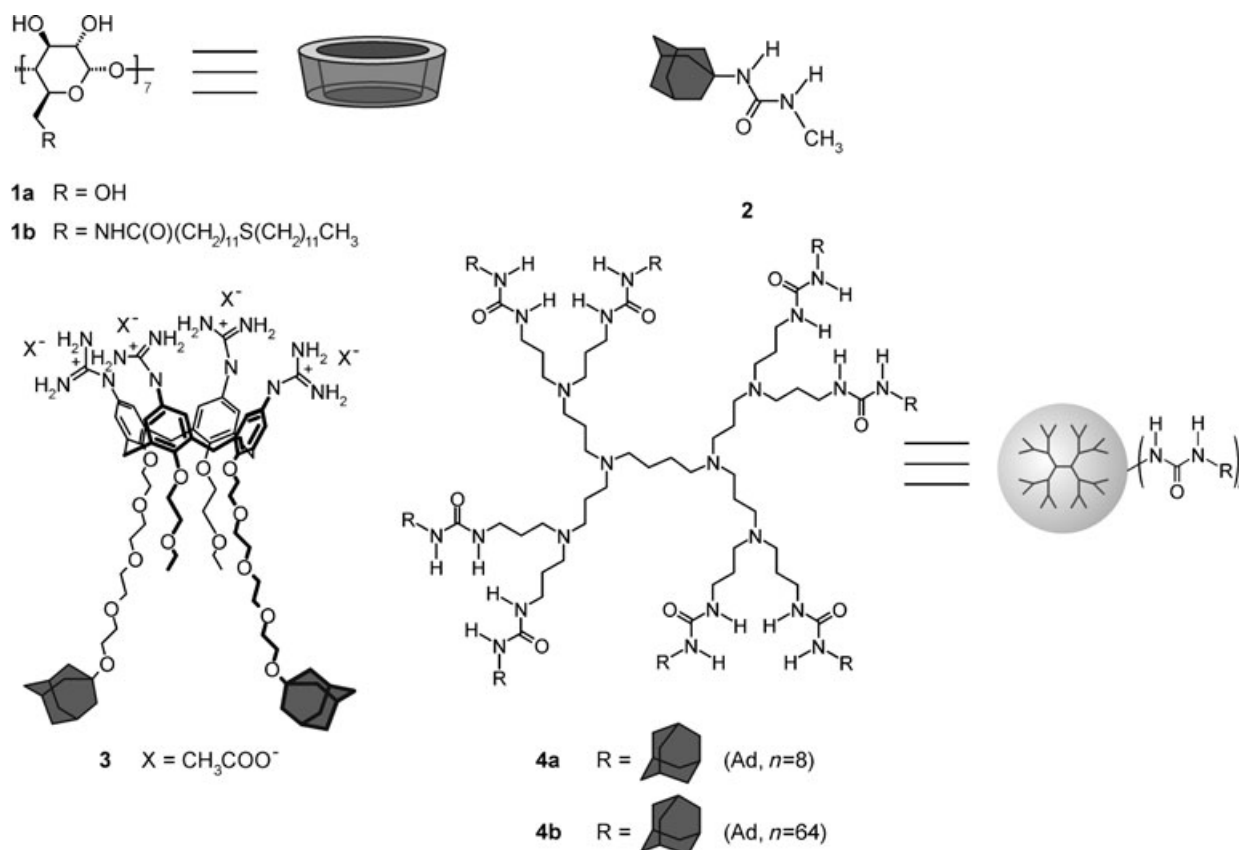
SAMs of the  $\beta$ -CD heptathioether adsorbate **1b** (Scheme 1) were prepared on gold layers (20 nm) on silicon substrates, as described previously by our group.<sup>[13,23]</sup> Scheme 1 also depicts the adamantyl- (Ad-) functionalized guest molecules (**2**, **3**, **4b**) that have been used in the present study for selective transfer onto the  $\beta$ -CD printboard on gold by supramolecular  $\mu$ CP and/or supramolecular DPN<sup>[22]</sup> (Figure 1).

### Supramolecular microcontact printing—pattern stability:

Our goal was to establish the dependence of the kinetic stability of the supramolecular patterns on the (multi)valency of the transferred (functional) molecules on the  $\beta$ -CD printboard during competitive rinsing with solutions that may contain an excess of the monovalent host, in our case native  $\beta$ -CD (**1a**).<sup>[15]</sup> Prior to studying the stability of the molecular patterns of **2**, **3**, and **4b** by AFM friction-force imaging, X-ray photoelectron spectroscopy (XPS) analysis<sup>[24]</sup> was performed to study the degree of guest deposition by adsorption from solution and by transfer from poly(dimethylsiloxane) (PDMS) stamps. For this purpose, divalent guest **3** was deposited on the entire surface of the  $\beta$ -CD printboard by printing with featureless PDMS stamps and by adsorption from solution. Physisorption due to electrostatic interactions was eliminated by rinsing the substrates with 50 mM aqueous NaCl solution (200 mL) and water (50 mL). XPS analysis of the bare  $\beta$ -CD printboard confirmed the presence of all elements (C, N, O, and S) in close-to-theoretical amounts (Table 1).

The amounts of guest present on the printboards were estimated by comparing experimental atomic compositions with the corresponding calculated values. The latter relate to a number of guest monolayers, in which a guest monolayer is defined as the amount of guest that leads to full saturation of available host sites by using the highest possible valency. For **3**, this corresponds to divalent binding.<sup>[18]</sup> To correct for the small deviations in atomic composition of the bare  $\beta$ -CD printboard between experimental and calculated values, the (absolute) changes in atomic composition were taken for comparison. Of the clear trends shown in Table 1, the carbon and oxygen data appeared to offer the best estimation.

Adsorption from solution ( $\Delta$ C %  $-1.7$ ,  $\Delta$ O %  $+0.9$ ) resulted in approximately one monolayer of guest molecules



Scheme 1. Chemical structures of the receptors,  $\beta$ -cyclodextrin (**1a**) and the  $\beta$ -CD adsorbate for attachment to gold (**1b**), and of the guests, 1-adamantyl-3-methyl-urea (**2**), bis(adamantyl)-functionalized calix[4]arene (**3**), and the fifth-generation adamantyl-functionalized poly(propylene imine) dendrimer (G5-PPI-(Ad)<sub>64</sub>, **4b**). The chemical structure of G2-PPI-(Ad)<sub>8</sub> (**4a**) is shown for convenience.

on the surface (expected:  $\Delta C\%$   $-1.8$ ,  $\Delta O\%$   $+0.9$ ), while the N and S changes were also in close agreement. Conversely, the experimental values indicate that 1) up to 5 guest monolayers (expected:  $\Delta C\%$   $-5.0$ ,  $\Delta O\%$   $+4.5$ ) were transferred during physical contact of the stamp with the printboard ( $\Delta C\%$   $-5.2\%$ ,  $\Delta O\%$   $+2.7$ ) and 2) 1–2 guest monolayers ( $\Delta C\%$   $-2.8$ ,  $\Delta O\%$   $+2.3$ ) remained after rinsing the substrate with 50 mM aqueous NaCl (200 mL; expected:  $\Delta C\%$   $-3.0$ ,  $\Delta O\%$   $+1.6$ ). Submonolayer coverages resulted after rinsing with competitive rinsing solutions (for example, 1–10 mM native  $\beta$ -CD at pH 2, data not shown).

The stability of the molecular patterns of a series of different guest molecules was studied by comparing the patterns on the  $\beta$ -CD printboard directly after  $\mu$ CP with the patterns after rinsing with water, 1 mM  $\beta$ -CD, or 10 mM  $\beta$ -CD solutions (200 mL; Figures 2 and 3). By contact-mode AFM imaging of the  $\beta$ -CD printboard after  $\mu$ CP, clear patterns of different friction contrast were observed; these patterns confirmed that the transfer of the guest molecules from the PDMS stamp onto the substrates had taken place (Figure 2a,d).<sup>[25]</sup>

Rinsing with water resulted in the complete removal of the patterns of monovalent guest **2** from the  $\beta$ -CD printboard, as shown by the disappearance of the friction contrast (Figure 2a,b). This rinsing procedure did not affect the

patterns of divalent guest **3** (Figure 2d,e). Moreover, even rinsing with substantial amounts of 10 mM  $\beta$ -CD solution did not result in complete removal of the patterns of **3** (Figure 2f), even though competition is known to enhance multivalent dissociation kinetics.<sup>[26]</sup> The high stability of the molecular patterns of **3** to rinsing with 10 mM  $\beta$ -CD solution stems from the high overall interaction strength if a guest is capable of forming more than one supramolecular interaction with  $\beta$ -CDs on the printboard.<sup>[18,19]</sup> On a qualitative basis, it is clear from the relative friction contrast changes before and after rinsing with 10 mM  $\beta$ -CD solution, that molecular patterns of multivalent guest **4b** (Figure 3a,c) are even more stable towards competitive rinsing than the divalent guest **3** (Figure 2d,f).

The fact that the transfer of **4b**, as its per- $\beta$ -CD complex,<sup>[27]</sup> by  $\mu$ CP onto the  $\beta$ -CD printboard is successful and the fact that its patterns are very stable during competitive rinsing emphasize its strongly multivalent nature, with association most probably occurring through seven Ad-CD interactions, as has been recently shown for similar ferrocenyl-functionalized dendrimers.<sup>[21]</sup> AFM height measurements (not shown) illustrate that during  $\mu$ CP, multilayers of guest **4b** (feature height about 3 nm) were transferred onto the  $\beta$ -CD printboard. Friction contrast variations within the areas of transfer (Figure 3a,d) correlate with nonuniformities in

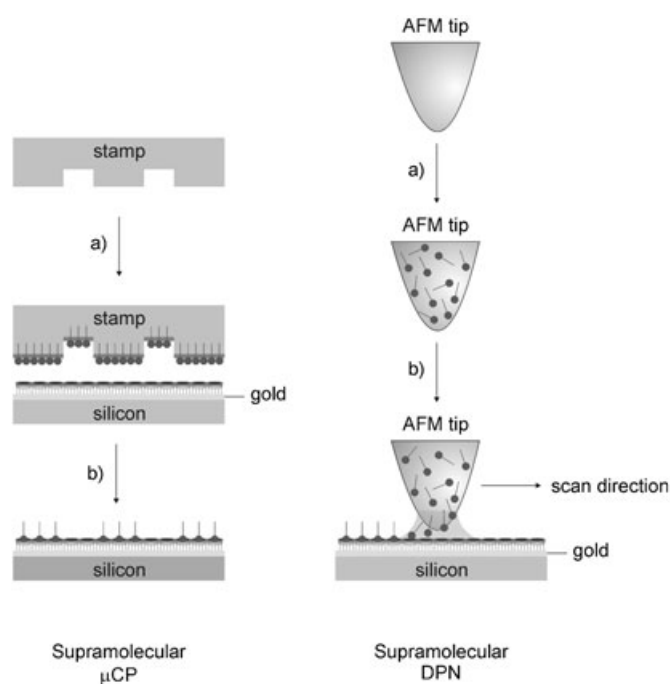


Figure 1. Schematic representation of supramolecular  $\mu$ CP and supramolecular DPN of printboard-compatible guests on the  $\beta$ -CD printboard on gold. Left: supramolecular  $\mu$ CP: a) PDMS stamps are fabricated from a master by replica molding (REM) of, in our case, a silicon master structure with regular lines of 5  $\mu$ m width, 10  $\mu$ m spacing, and 1.2  $\mu$ m depth. Treatment of the PDMS stamps by mild oxidation in a UV/ozone plasma reactor for 60 min is followed by immersion in an aqueous solution of the guest for about 15–30 min in order to ink the stamp; b) contact-printing experiments on the  $\beta$ -CD printboard are carried out by hand for 1–2 min. For our pattern stability study, the substrates are rinsed with substantial amounts of aqueous solutions. Right: supramolecular DPN: a) clean silicon nitride AFM tips are wet-inked by immersing the tips for 15 min in an aqueous solution of the guest; b) writing experiments on the  $\beta$ -CD printboard are carried out in an ambient atmosphere ( $T=25^\circ\text{C}$ , relative humidity = 40–50%) by scanning the tip in contact mode along a line on the substrate for a certain period of time.

Table 1. Elemental analysis by XPS of the bare  $\beta$ -CD printboard versus printboards onto which divalent guest **3** was deposited by adsorption from solution or by  $\mu$ CP, and calculated XPS values relating to the number of monolayers of **3** present on the printboard.

		XPS [percentage composition]			
		C(1s)	N(1s)	O(1s)	S(2p)
experimental	guest deposition				
	no guest (bare $\beta$ -CD)	79.5 $\pm$ 0.9	2.6 $\pm$ 0.5	16.2 $\pm$ 0.4	1.7 $\pm$ 0.1
	adsorption	77.8 $\pm$ 0.6	4.0 $\pm$ 0.3	17.1 $\pm$ 0.6	1.2 $\pm$ 0.3
	$\mu$ CP	74.5 $\pm$ 0.7	3.7 $\pm$ 0.2	20.7 $\pm$ 1.0	1.1 $\pm$ 0.2
	$\mu$ CP + rinsing	76.7 $\pm$ 0.5	3.6 $\pm$ 0.4	18.5 $\pm$ 0.9	1.3 $\pm$ 0.1
calculated	no. of monolayers of <b>3</b> <sup>[a]</sup>				
	0 (bare $\beta$ -CD)	81.0	2.7	13.5	2.7
	1	79.2	4.1	14.4	2.2
	2	78.0	5.0	15.1	1.9
	3	77.1	5.7	15.6	1.6
	4	76.4	6.3	16.0	1.4
	5	75.8	6.7	16.2	1.3

[a] One monolayer of guest **3** is defined as consisting of a 2:1 CD:**3** stoichiometry with the  $\beta$ -CD printboard in order to reflect the interaction of both adamantyl functionalities with the  $\beta$ -CD printboard.

layer thickness. Rinsing with 10 mM  $\beta$ -CD solution only resulted in the removal of physisorbed **4b**, leaving approximately one monolayer of **4b** on the  $\beta$ -CD printboard (feature height after rinsing, about 1 nm). Apparently, the interaction strength of guest **4b** with the  $\beta$ -CD printboard is sufficient to apply our receptor surfaces as molecular printboards for the printing of stable molecular patterns of multivalent guests by supramolecular  $\mu$ CP.

EIS measurements were carried out in order to obtain more information on the degree of deposition of guest **4b** on the printboard. For this purpose, multivalent guest **4b** was deposited on the entire surface of  $\beta$ -CD printboards by printing with featureless PDMS stamps and by adsorption from solution. The effect of rinsing with 10 mM CD solution (200 mL) at pH 2 and water (50 mL) at pH 2 was also taken into account (Table 2).

The initial charge-transfer resistance ( $R_{CT}$ ) of the  $\beta$ -CD printboard (42 k $\Omega$ ) towards the negatively charged  $[\text{Fe}(\text{C}-\text{N})_6]^{4-}/[\text{Fe}(\text{CN})_6]^{3-}$  reporter redox couple is similar to  $R_{CT}$  values reported previously by our group<sup>[13]</sup> and reflects a high degree of order of this monolayer to block the redox current to the gold efficiently. The presence of guest **4b** on the printboard is known to significantly decrease this  $R_{CT}$  value, since electrostatic attraction of the anionic reporter redox couple with the positively charged dendritic core facilitates the oxidation/reduction at the electrode surface.<sup>[9]</sup> This was found to be the case for deposition of **4b** onto the printboard by adsorption from solution or by  $\mu$ CP and subsequent rinsing (7–8 k $\Omega$ ), the process resulting in monolayer coverages of guest molecules on the printboard. Conversely, a twofold increase in the  $R_{CT}$  value upon deposition by  $\mu$ CP (without rinsing) suggests, in agreement with the AFM analysis, the transfer of multilayers of guest **4b** onto the  $\beta$ -CD printboard during  $\mu$ CP. In this case, the increase of the layer thickness of guest molecules on top of the printboard impedes the redox current to the electrode surface and, therefore, results in a higher  $R_{CT}$  value.

To rule out any interference from nonspecific interactions on the  $\beta$ -CD printboard, printing experiments under the same conditions were carried out on SAMs of 11-mercaptoundecanol (OH SAMs). OH SAMs were chosen as reference layers, since these SAMs have a similar polarity to that observed for SAMs of  $\beta$ -CD, but are incapable of forming inclusion complexes with the guest molecules. Figure 3a–f illustrates the concept of the molecular printboard by the difference in stability of the patterns of multivalent guest **4b** on the  $\beta$ -CD printboard and OH SAMs upon subsequent rinsing with different concentrations of  $\beta$ -CD solutions.

Again, patterns with a clear friction contrast are apparent in contact-mode AFM images of the OH SAM after  $\mu$ CP. This indicates that the transfer of guest molecules from the stamp onto the  $\beta$ -CD printboard does not rely on specific interactions, but that physical contact is sufficient to generate patterns of molecules (Figure 3a, d). The requirement of *specific* supramolecular interactions for the stability of the molecular patterns on the printboard is, however, evident from the complete removal of the patterns of multivalent

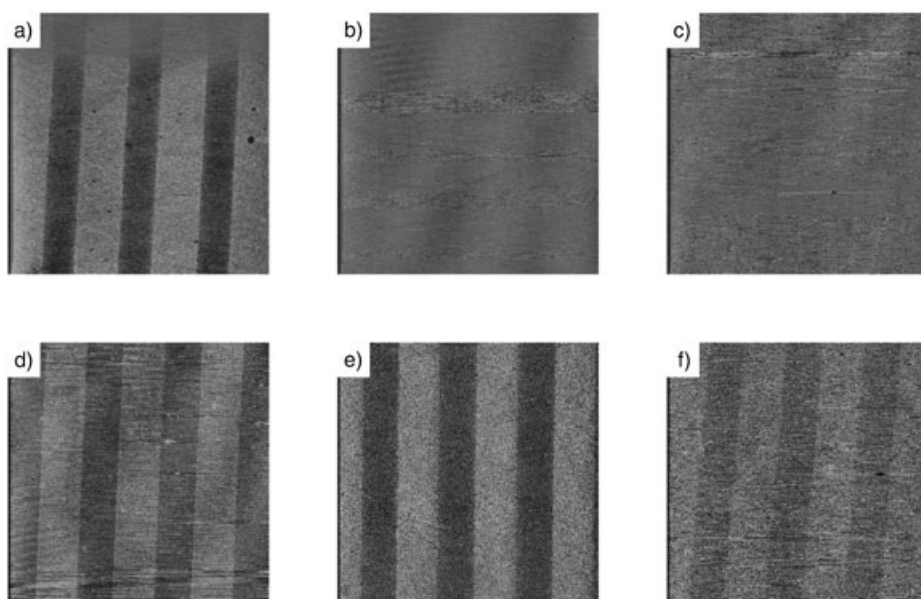


Figure 2. Contact-mode AFM friction images acquired in air of patterns of monovalent guest **2** (top) and divalent guest **3** (bottom) showing patterns present: a,d) after  $\mu$ CP of the guests (brighter areas) on the  $\beta$ -CD printboard, b,e) after rinsing with water, and c,f) after rinsing with 10 mM  $\beta$ -CD at pH 2 (image sizes  $50 \times 50 \mu\text{m}^2$ ; friction forces [a.u.] increase from dark to bright contrast).

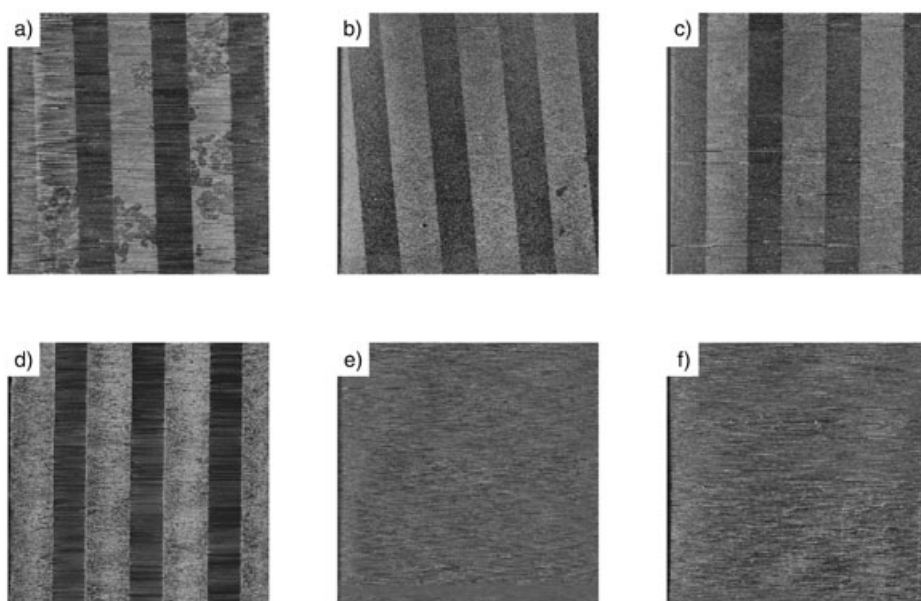


Figure 3. Contact-mode AFM friction images acquired in air of micrometer-size line patterns of multivalent guest **4b** (brighter areas) on the  $\beta$ -CD (top) and 11-mercaptoundecanol (bottom) SAMs showing patterns present: a,d) after  $\mu$ CP of the guest, b,e) after rinsing with 1 mM  $\beta$ -CD at pH 2, and c,f) after rinsing with 10 mM  $\beta$ -CD at pH 2 (image sizes  $50 \times 50 \mu\text{m}^2$ ; friction forces [a.u.] increase from dark to bright contrast).

guest **4b** from the OH SAMs upon rinsing with 1 mM and 10 mM  $\beta$ -CD solutions (Figure 3e,f), a result confirming physisorption in this case. Patterns of **4b** on the  $\beta$ -CD printboards were stable, even after rinsing with substantial amounts of 10 mM  $\beta$ -CD solution (Figure 3c).

Poly(propylene imine) (PPI) dendrimers such as **4b** have already been employed by our group as nanocontainers for

dye molecules on the  $\beta$ -CD printboard<sup>[28]</sup> and as water-soluble nanoreactors for the formation of gold nanoparticles in solution.<sup>[29]</sup> In the present study, the latter dendrimer-stabilized gold nanoparticles were exploited to facilitate the fabrication of metal patterns on the printboard by incorporating an additive technique, namely electroless deposition (ELD), into our supramolecular patterning strategies.

#### Electroless deposition—fabrication of metal patterns on the printboard: ELD<sup>[30]</sup>

ELD<sup>[30]</sup> is a routine and cost-effective fabrication technique for the selective deposition of metal on surfaces. It is an autocatalytic redox process that comprises the reduction and deposition of metallic ions (as the source of metal) from solution to a substrate in the presence of a reducing agent. To initiate ELD of metal onto surfaces, the only requirement is a surface containing a catalyst. For this purpose, gold nanoparticles stabilized by fifth-generation (G5) PPI dendrimers were prepared, as reported previously by our group,<sup>[29]</sup> and subsequently transferred as catalysts for ELD onto the molecular printboard by supramolecular  $\mu$ CP. Figure 4a,b shows AFM height images before and after immersion of this printboard in a copper ELD bath for 5 min. The heights, observed at these stages and averaged over relatively large feature areas, were 2 and 64 nm, respectively (see the cross-section AFM analysis in Figure 4).

The fact that the patterns of dendrimer-stabilized nanoparticles were stable during competitive rinsing with 10 mM  $\beta$ -CD at pH 2 (Figure 4a) supports the idea that the gold particles reside inside the dendrimers.<sup>[29]</sup> Stability of these patterns is afforded through multivalent interactions of several Ad functionalities at the outer interface of the dendrimers with the printboard. As argued before, the dense, insulating shell of supramolecular Ad- $\beta$ -CD complexes protects the

Table 2. EIS results of the bare  $\beta$ -CD printboard versus printboards onto which multivalent guest **4b** was deposited by adsorption from solution or by  $\mu$ CP.

Guest deposition	$R_{CT}^{[a]}$ [k $\Omega$ ]
no guest	42
adsorption	8.4
$\mu$ CP	75
$\mu$ CP + rinsing	7.3

[a] Charge-transfer resistance towards  $[\text{Fe}(\text{CN})_6]^{4-}/[\text{Fe}(\text{CN})_6]^{3-}$ .

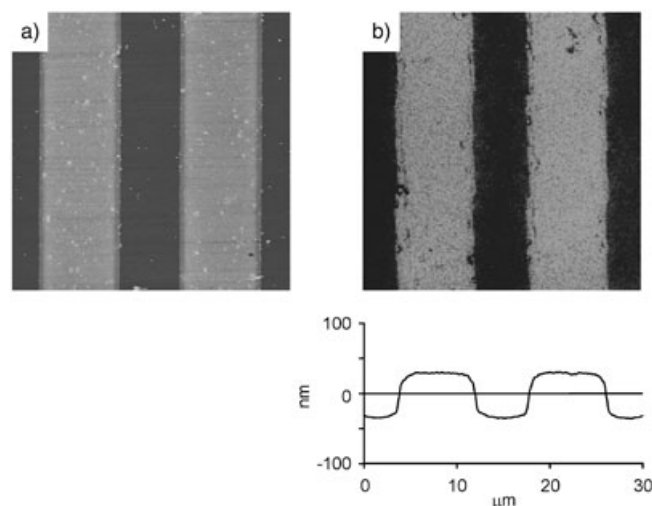


Figure 4. Contact-mode AFM height images acquired in air of patterns (image sizes  $30 \times 30 \mu\text{m}^2$ ) of a) gold nanoparticles stabilized by G5-PPI dendrimers, deposited on the  $\beta$ -CD printboard by supramolecular  $\mu$ CP and subsequently rinsed with 10 mM  $\beta$ -CD solution at pH 2, and b) copper structures obtained after subsequent electroless deposition (ELD) on the dendrimer-patterned printboard for 5 min.

nanoparticles inside the dendrimer from coagulation.<sup>[29]</sup> The ELD experiment shown here illustrates that these nanoparticles are still accessible to act as catalytic centers for the electroless deposition of copper. Figure 4b also illustrates the high selectivity for copper deposition in the target areas containing the dendrimer-stabilized gold nanoparticles. The direct placement of these catalytic centers and the protective nature of the  $\beta$ -CD SAM for the underlying gold substrate accounts for this observation.

The combination of ELD and  $\mu$ CP has been reported previously to offer a routine and cost-effective fabrication technique for metal patterns.<sup>[31,32]</sup> However, the distinct difference between our work and these previous reports is the use of multivalent supramolecular interactions between the catalyst and the surface that can subsequently serve as a strong connection between the metal patterns and the substrate.

**Supramolecular DPN—writing local molecular patterns at the sub-100-nm scale:** DPN is a promising lithographic technique that allows the extension of our supramolecular patterning strategy on the printboard to the sub-100-nm scale (Figure 1).<sup>[6,7]</sup> Previously, we have shown that patterns of **3** on the  $\beta$ -CD printboard transferred by DPN are similar to

those prepared by supramolecular  $\mu$ CP, with regard to the issues of ink transfer and pattern stability upon rinsing.<sup>[22]</sup> To investigate the potential of supramolecular DPN, the lateral resolution was investigated by writing patterns with different width-to-length ratios (Figure 5a).<sup>[33]</sup>

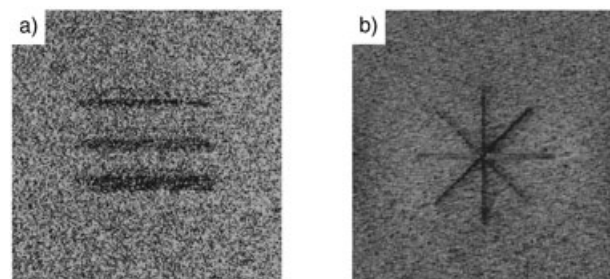


Figure 5. Contact-mode AFM friction images acquired in air of patterns present on the  $\beta$ -CD printboard: a) An array of lines,  $7 \mu\text{m}$  long with mean widths ( $\pm$  standard deviation) of  $290 \pm 20$ ,  $480 \pm 30$ , and  $880 \pm 50$  nm, of divalent guest **3** after scanning the tip at a velocity of  $\approx 21 \mu\text{m s}^{-1}$  across the  $\beta$ -CD printboard for 10 min for each line (image size  $15 \times 15 \mu\text{m}^2$ ; friction forces [a.u.] increase from dark to bright contrast). b) An array of lines,  $3 \mu\text{m}$  long with average widths of approximately  $60 \pm 20$  nm, of multivalent guest **4b** after scanning the tip at a velocity of  $\approx 4 \mu\text{m s}^{-1}$  across the  $\beta$ -CD printboard for 10 min for each line (image size  $6 \times 6 \mu\text{m}^2$ ; friction forces [a.u.] increase from dark to bright contrast). Readout of the patterns was done with the same tip by increasing the scan size and the scan velocity (approximately 15 times the writing speed).

Figure 5a shows a friction AFM image of a pattern of **3** consisting of three rectangles,  $7 \mu\text{m}$  long with targeted widths of 220, 440, and 880 nm (top to bottom), respectively, written by DPN on the  $\beta$ -CD printboard over 10 min for each rectangle. Inversion of the relative friction contrast in the image in comparison to that observed in Figure 2 is probably related to the different character of the contacting surfaces (that is, ink-covered tip versus bare tip). This has been observed before for similar  $\beta$ -CD systems,<sup>[22]</sup> as well as for polyamidoamine (PAMAM) dendrimers on other SAMs.<sup>[34]</sup>

Overinking during the writing stage and the effect of instrumental drifts are parameters that could cause the pattern broadening in this particular experiment to be more significant at high-resolution writing (approximately 30% for the 220-nm line, 10% for the 440-nm line). The sub-100-nm writing capability of supramolecular DPN is shown in Figure 5b with an array of lines of guest **4b** on the printboard with a line width of 60 nm. In addition to writing regular line patterns, this specific pattern was written in three stages by adjusting the scan angle of the tip by  $45^\circ$  each time with respect to the previous line. In this particular experiment, gold-coated tips functionalized with a poly(ethylene glycol) SAM were used to allow a better transfer of **4b** to the printboard. Scanning with a bare, uninked silicon nitride AFM tip over the  $\beta$ -CD printboard under the same experimental conditions did not form any visible pattern, thus proving that pattern formation arises from the transfer of guest mol-

ecules and not from mechanical forces applied by the tip to the printboard.

## Conclusion

The results herein demonstrate the successful application of micro- and nanopatterning strategies, supramolecular  $\mu$ CP and supramolecular DPN, respectively, that employ the concept of the molecular printboard.

Supramolecular  $\mu$ CP with guests of different valency was carried out on the  $\beta$ -CD printboard for testing the stability of the patterns during rinsing with substantial amounts of water and competitive aqueous solutions. It was found that all kinetic stabilities can be observed: rapid removal by water in case of a monovalent guest, slower partial removal by competitive rinsing in case of a divalent guest, and complete stability for truly multivalent guests. Interference of nonspecific interactions in the formation of molecular patterns on the printboard was ruled out by the complete removal of the molecular pattern during mild rinsing conditions on reference OH SAMs. Clearly, the novelty of our patterning strategy over existing fabrication strategies for molecular patterns on substrates lies in the tunable pattern stability of printboard-compatible guests on the molecular printboard through the use of specific, multivalent supramolecular interactions.

Supramolecular DPN was exploited on the  $\beta$ -CD printboard to extend our supramolecular patterning strategy into the sub-100-nm range, as shown by the nanoscale patterns with 60 nm line width.

Electroless deposition of metal patterns on the printboard demonstrated that molecular printboards constitute a useful tool for the fabrication and application of supramolecular architectures on surfaces.

## Experimental Section

**Chemicals and substrates:** The synthesis of the  $\beta$ -CD heptathioether adsorbate and the preparation of SAMs on gold substrates were reported previously by our group.<sup>[13,23]</sup> The syntheses of the fifth-generation adamantane-terminated poly(propylene imine) dendrimer (G5-PPI-(Ad)<sub>64</sub>) and its per- $\beta$ -CD complex were carried out according to literature procedures.<sup>[28]</sup> Gold layers (20 nm) on titanium-primed (2–3 nm) silicon wafers were purchased from Ssens BV (Hengelo, The Netherlands). 11-Mercapto-undecanol and native  $\beta$ -cyclodextrin were purchased from Aldrich and Acros, respectively, and used without further purification. Solvents used for monolayer preparation were of p.a. grade.

**1-Adamantyl-3-methyl-urea (2):** 1-Adamantyl isocyanate (0.5 g, 2.8 mmol) was added to a solution of methylamine (0.105 g, 3.4 mmol) in chloroform (20 mL). This mixture was stirred overnight at room temperature under argon. The solvent was removed under vacuum. Subsequently, diethyl ether was added to the residue to isolate the product as a white solid (0.260 g, 1.25 mmol; 45 %): <sup>1</sup>H NMR (300 MHz, CDCl<sub>3</sub>):  $\delta$  = 4.13 (brs, 1H), 4.09 (brs, 1H), 2.71 (d,  $J$  = 5.1 Hz, 2H), 2.09–2.03 (m, 3H; CH<sub>2</sub>CHCH<sub>2</sub>[Ad]), 1.98–1.94 (m, 6H; CHCH<sub>2</sub>C[Ad]), 1.68–1.64 ppm (m, 6H; CHCH<sub>2</sub>CH[Ad]); <sup>13</sup>C NMR (100 MHz, CDCl<sub>3</sub>):  $\delta$  = 158.24, 50.75, 42.58, 36.48, 29.60, 26.89 ppm; FAB-MS:  $m/z$  calcd for  $[M+H]^+$ : 209.2; found: 209.2.

**Substrate and monolayer preparation:** Prior to use, all glassware was cleaned by immersion in piranha (3:1 ratio of conc. H<sub>2</sub>SO<sub>4</sub> and 33 wt % H<sub>2</sub>O<sub>2</sub>) for 30 min and rinsing with substantial amounts of water. Gold substrates of 1 × 1 cm<sup>2</sup> were cleaned by oxygen plasma treatment for 5 min and the resulting oxide layer was reduced by leaving the substrates for 10 min in absolute EtOH.<sup>[35]</sup> Subsequently, the clean gold substrates were immersed in an adsorbate solution (0.1–1.0 mM) with minimal delay for approximately 16 h. After incubation, the substrates were rinsed with substantial amounts of dichloromethane, ethanol, and water.

**Supramolecular microcontact printing:** Stamps were fabricated by casting a 10:1 (v/v) mixture of PDMS and curing agent (Sylgard 184, Dow Corning) against a photolithographically patterned silicon master, cured for 1 h at 60 °C, and released at this curing temperature to avoid buildup of tension due to thermal shrinkage.<sup>[36]</sup> PDMS stamps, used for  $\mu$ CP, were left in the oven at 60 °C for at least 18 h to ensure complete curing.

Oxidation of PDMS stamps was carried out in a commercial UV/ozone plasma reactor (Ultra-Violet Products Inc., model PR-100) for 60 min at a distance of about 2 cm from the plasma source. This type of reactor contains a low-pressure mercury UV light operating with UV emissions at 185 nm (1.5 mWcm<sup>-2</sup>) and 254 nm (15 mWcm<sup>-2</sup>) to generate molecular oxygen. UVO treatment<sup>[37]</sup> of the PDMS stamp was chosen over other techniques<sup>[38,39,40]</sup> because it is one of the milder treatments that results in similarly drastic changes of the surface chemical properties of the PDMS to those observed with, for example, oxygen plasma treatment and it provides surfaces that were found to be more resistant towards mechanical stress (that is, crack formation<sup>[41]</sup>) during  $\mu$ CP. The PDMS stamps were kept hydrophilic by immersing the stamps in an aqueous ink solution immediately after UVO treatment and in between the prints.<sup>[42]</sup> Hydrophobic recovery of PDMS after the UVO treatment<sup>[43]</sup> restricts the use of this type of surface modification for  $\mu$ CP<sup>[44]</sup> and was, therefore, monitored by contact-angle measurements over time. UVO-exposed PDMS is moderately hydrophilic ( $\theta_{adv}$  = 68°) after 1 h of UVO treatment and retains part of its hydrophilic character for at least several hours ( $\Delta\theta_{adv}$   $\approx$  10° after 4 h) if it is kept under water. Thereafter, this hydrophobic recovery was found to level off, as observed by the contact-angle increase of about 4° within the next 20 h. For reproducibility, all printing experiments were carried out within the first 4 h after UVO treatment, without reactivation of the stamps.

Subsequently, the stamps were inked by immersion into the adsorbate solution (0.1–1.0 mM in hydrophobic constituents) for 15–30 min. After withdrawal from the solution and drying under a continuous stream of nitrogen for 1 min, the stamps were applied by hand for 1–2 min on the substrate (the  $\beta$ -CD printboard or reference 11-mercapto-1-undecanol SAM). Reinking was done after each printing step. Finally, the substrates were systematically rinsed with aqueous solutions (200 mL) of native  $\beta$ -CD (1 or 10 mM at pH 2), NaCl (50 mM), or Milli-Q water. Additional rinsing with Milli-Q water was done in the first two cases in order to remove any excess of  $\beta$ -CD or salt on the printboard.

**Supramolecular DPN:** Si<sub>3</sub>N<sub>4</sub> tips were cleaned in chloroform overnight and inked by immersion into the adsorbate solution (0.5–1.0 mM in hydrophobic constituents) with minimal delay for 15 min. After withdrawal and drying, the tip was scanned in contact mode across the surface of the  $\beta$ -CD printboard for a certain period of time ( $T$  = 25 °C, relative humidity = 40–50 %). The written patterns were recorded with the same tip by increasing the scan size and the scan velocity (approximately 15 times the writing speed).

**Electroless deposition (ELD) of copper:** To trigger the ELD of Cu on the printboard, gold nanoparticles stabilized by the G5-PPI dendrimers were prepared according to a literature procedure<sup>[29]</sup> and transferred onto the printboard by conducting supramolecular  $\mu$ CP. After rinsing with an aqueous solution (200 mL) of native  $\beta$ -CD (10 mM at pH 2) and with Milli-Q water (200 mL), the substrate was immersed in the copper electroless-deposition bath containing 40 mM CuSO<sub>4</sub>, 140 mM Na<sub>2</sub>SO<sub>4</sub>, 120 mM ethylenediaminetetraacetate sodium salt (Na<sub>4</sub>EDTA), 300 mM NaHCOO, and 30 mM HCHO at pH 13. After a certain immersion time, the substrate was taken out of the ELD bath, rinsed with Milli-Q water, and dried under a continuous stream of nitrogen for 1 min.

**Characterization:** AFM analyses were carried out with a NanoScope III multimode atomic force microscope (Veeco/Digital Instruments, Santa Barbara, CA, USA) equipped with a J-scanner, in contact mode by using  $\text{Si}_3\text{N}_4$  cantilevers (Nanoprobes, Veeco/Digital Instruments) with a nominal spring constant of  $0.1 \text{ Nm}^{-1}$ . To ensure maximum sensitivity for lateral forces in the friction-force images, the sample was scanned at  $90^\circ$  with respect to the long axis of the cantilever. AFM imaging was done in an ambient atmosphere ( $T=25^\circ\text{C}$ , relative humidity = 40–50 %).

XPS analyses were carried out with a Physical Electronics Quantum2000 apparatus equipped with an Al  $K\alpha$  monochromatic excitation source (source energy = 1486.7 eV, take-off angle set to  $30^\circ$ ), a spherical sector analyzer, and a multichannel plate detector (16 detector elements). For the survey scan (pass energy of 117 eV), the X-ray beam was set to high power mode (100 W per  $100 \mu\text{m}$ ) to scan a total area of  $1000 \times 500 \mu\text{m}$ ; for element scans (pass energy of 29.35 eV), the X-ray beam was set to 25 W per  $100 \mu\text{m}$  to scan a total area of  $1000 \times 500 \mu\text{m}$  (298 K and  $1\text{--}3 \times 10^{-8}$  Torr). The sensitivity factors used for C, N, O, and S in the calculation of the atomic concentration were 0.314, 0.499, 0.733, and 0.717, respectively. The hydrocarbon C(1s) signal at 284.8 eV was used as the reference to correct for surface charging.

Electrochemical impedance spectroscopy measurements were carried out with an AUTOLAB PGSTAT10 apparatus (ECONCHEMIE, Utrecht, The Netherlands) in a custom-built three-electrode setup consisting of a platinum counterelectrode, a mercurous sulfate reference electrode (MSE;  $V_{\text{MSE}} = 0.61 V_{\text{normal hydrogen electrode}}$ ), and a gold working electrode (held by a screw cap to the bottom of the cell and exposing a geometric area of  $0.44 \text{ cm}^2$  to the electrolyte solution). Scans were carried out by using a frequency range from 10 kHz to 0.1 Hz in  $1 \text{ mM K}_3\text{Fe}(\text{CN})_6/\text{K}_4\text{Fe}(\text{CN})_6$  containing  $0.1 \text{ M K}_2\text{SO}_4$  at  $-0.2 V_{\text{MSE}}$  with a 5 mV amplitude. The charge-transfer resistance ( $R_{\text{CT}}$ ) of the monolayer was determined from the Nyquist plot by fitting the experimental data to an equivalent Randles circuit containing a charge-transfer resistance of the monolayer in parallel with the capacitance of the monolayer and in series with the resistance of the solution.<sup>[45]</sup>

NMR spectroscopy was carried out at  $25^\circ\text{C}$  by using a Varian Unity Inova 300 spectrometer or a Varian Unity 400 WB spectrometer.  $^1\text{H}$  NMR (300 MHz) and  $^{13}\text{C}$  NMR (100 MHz) chemical shifts are given relative to residual  $\text{CHCl}_3$  ( $\delta = 7.27$  and  $77.0$  ppm, respectively).

FAB mass spectrometry was carried out with a Finnigan MAT90 spectrometer with *m*-nitrobenzyl alcohol (NBA) as the matrix.

## Acknowledgements

A. H. J. van den Berg of the CMAL/MESA<sup>+</sup> Institute for Nanotechnology is acknowledged for XPS analysis of the substrates. Dr. Andrea Sartori, Prof. A. Casnati, and Prof. R. Ungaro of the University of Parma are acknowledged for the synthesis of the bis(adamantyl)-functionalized calix[4]arene guest molecule **3**. Financial support for this work was given by the MESA<sup>+</sup> Institute for Nanotechnology (Strategic Research Orientation 'Advanced Photonic Structures'), by the Council for Chemical Sciences of the Netherlands Organization for Scientific Research (NWO-CW: grants 700.97.041 (B.D. and T.A.), 700.50.522 Young Chemists program (O.C.-B.) to J.H., 700.98.305 (A.M.), and vernieuwingsimpuls grant to H.S.), and by the Dutch Technology Foundation STW (grant TST4946 (M.P. and C.A.N.) to D.N.R.). The partial support of the EC-funded project NaPa (contract NMP4-CT-2003-500120) is gratefully acknowledged. The content of this work is the sole responsibility of the authors.

- [1] a) Y. Xia, G. M. Whitesides, *Angew. Chem.* **1998**, *110*, 568–594; *Angew. Chem. Int. Ed.* **1998**, *37*, 550–575; .  
 [2] B. Michel, A. Bernard, A. Bietsch, E. Delamarche, M. Geissler, D. Juncker, H. Kind, J.-P. Renault, H. Rothuizen, H. Schmid, P. Schmid-Winkel, R. Stutz, H. Wolf, *IBM J. Res. Dev.* **2001**, *45*, 697–719.

- [3] S. Krämer, R. R. Fuieler, C. B. Gorman, *Chem. Rev.* **2003**, *103*, 4367–4418.  
 [4] A. Bernard, J.-P. Renault, B. Michel, H. R. Bosshard, E. Delamarche, *Adv. Mater.* **2000**, *12*, 1067–1070.  
 [5] L. Yan, W. T. S. Huck, X.-M. Zhao, G. M. Whitesides, *Langmuir* **1999**, *15*, 1208–1214.  
 [6] M. Jäschke, H.-J. Butt, *Langmuir* **1995**, *11*, 1061–1064.  
 [7] a) R. D. Piner, J. Zhu, F. Xu, S. Hong, C. A. Mirkin, *Science* **1999**, *283*, 661–663; b) C. A. Mirkin, S. Hong, R. D. Levine, *ChemPhys-Chem* **2001**, *2*, 37–39.  
 [8] L. M. Demers, D. S. Ginger, S.-J. Park, Z. Li, S.-W. Chung, C. A. Mirkin, *Science* **2002**, *296*, 1836–1838.  
 [9] J. Huskens, M. A. Deij, D. N. Reinhoudt, *Angew. Chem.* **2002**, *114*, 4647–4651; *Angew. Chem. Int. Ed.* **2002**, *41*, 4467–4471; .  
 [10] J. Szejtli in *Comprehensive Supramolecular Chemistry, Vol. 3 Cyclodextrins* (Vol. Eds.: J. Szejtli, T. Osa), Pergamon Press, Oxford, **1996**, pp. 5–41 and pp. 189–205.  
 [11] M. V. Rekharsky, Y. Inoue, *Chem. Rev.* **1998**, *98*, 1875–1917.  
 [12] H. Schönherr, M. W. J. Beulen, J. Bügler, J. Huskens, F. C. J. M. Van Veggel, D. N. Reinhoudt, G. J. Vancso, *J. Am. Chem. Soc.* **2000**, *122*, 4963–4967.  
 [13] M. W. J. Beulen, J. Bügler, M. R. de Jong, B. Lammerink, J. Huskens, H. Schönherr, G. J. Vancso, A. Boukamp, H. Wieder, A. Offenhäuser, W. Knoll, F. C. J. M. Van Veggel, D. N. Reinhoudt, *Chem. Eur. J.* **2000**, *6*, 1176–1183.  
 [14] A. Ulman, *An Introduction to Ultrathin Organic Films*, Academic Press, San Diego, **1991**.  
 [15] M. R. de Jong, J. Huskens, D. N. Reinhoudt, *Chem. Eur. J.* **2001**, *7*, 4164–4170.  
 [16] Generally, a molecular printboard is a SAM of receptor molecules that have specific recognition sites, for example, molecular cavities, at which one can immobilize molecules from aqueous solutions through specific and directional supramolecular interactions.  
 [17] See guest **3** (Scheme 1). This calix[4]arene derivative has guanidinium functionalities at the upper rim to increase water solubility. Poly(ethylene glycol) (PEG) linkers at the lower rim space out the two adamantyl functionalities in order to allow this molecule to form inclusion complexes with two neighboring  $\beta$ -CDs on the  $\beta$ -CD SAM (lattice constant  $\beta$ -CD  $\approx 1.8 \text{ nm}$ ), while water solubility is retained and nonspecific interactions with the printboard are prevented.  
 [18] A. Mulder, T. Auletta, A. Sartori, S. Del Ciotto, A. Casnati, R. Ungaro, J. Huskens, D. N. Reinhoudt, *J. Am. Chem. Soc.* **2004**, *126*, 6627–6636.  
 [19] J. Huskens, A. Mulder, T. Auletta, C. A. Nijhuis, M. J. W. Ludden, D. N. Reinhoudt, *J. Am. Chem. Soc.* **2004**, *126*, 6784–6797.  
 [20] O. Crespo-Biel, M. Péter, C. M. Bruinink, B. J. Ravoo, D. N. Reinhoudt, J. Huskens, *Chem. Eur. J.* **2005**, *11*, 2426–2432.  
 [21] C. A. Nijhuis, J. Huskens, D. N. Reinhoudt, *J. Am. Chem. Soc.* **2004**, *126*, 12266–12267.  
 [22] T. Auletta, B. Dordi, A. Mulder, A. Sartori, S. Onclin, C. M. Bruinink, M. Péter, C. A. Nijhuis, H. Beijleveld, H. Schönherr, G. J. Vancso, A. Casnati, R. Ungaro, B. J. Ravoo, J. Huskens, D. N. Reinhoudt, *Angew. Chem.* **2004**, *116*, 373–377; *Angew. Chem. Int. Ed.* **2004**, *43*, 369–373.  
 [23] M. W. J. Beulen, J. Bügler, B. Lammerink, F. A. J. Geurts, E. M. E. F. Biemond, K. G. C. Van Leerdam, F. C. J. M. Van Veggel, J. F. J. Engbersen, D. N. Reinhoudt, *Langmuir* **1998**, *14*, 6424–6429.  
 [24] A. Benninghoven, *Angew. Chem.* **1994**, *106*, 1075–1096; *Angew. Chem. Int. Ed. Engl.* **1994**, *33*, 1023–1043.  
 [25] A drawback of surface modification of PDMS, including UV/ozone treatment for long periods of time ( $> 30 \text{ min}$ ), is that the formation of a thin silica-like surface layer ( $\text{SiO}_2$ ) changes the mechanical and adhesive properties of the stamp. The resulting change in deformation characteristics of the PDMS stamp under slight pressure, in order to make conformal contact between the stamp and the substrate, is the most probable cause affecting accurate pattern reproduction of the original stamp features ( $10 \mu\text{m}$  with  $5 \mu\text{m}$  spacing).



- See the printing results of line patterns (about 9  $\mu\text{m}$  with 6  $\mu\text{m}$  spacing, Figure 2 and Figure 3).
- [26] J. Rao, J. Lahiri, L. Isaacs, R. M. Weis, G. M. Whitesides, *Science* **1998**, *280*, 708–711.
- [27] Use of the per- $\beta$ -CD complex of **4b** is necessary to increase its water solubility (conditions: excess of native  $\beta$ -CD in water at pH 2) to obtain sufficiently concentrated ink solutions for  $\mu\text{CP}$  and DPN on the molecular printboard.
- [28] J. J. Michels, M. W. P. L. Baars, E. W. Meijer, J. Huskens, D. N. Reinhoudt, *J. Chem. Soc. Perkin Trans. 2* **2000**, 1914–1918.
- [29] J. J. Michels, J. Huskens, D. N. Reinhoudt, *J. Chem. Soc. Perkin Trans. 2* **2002**, 102–105.
- [30] G. O. Mallory, J. B. Hajdu, *Electroless Plating: Fundamentals and Applications*, American Electroplaters and Surface Finishers Society, Orlando, FL, **1990**.
- [31] A. M. Bittner, X. C. Wu, K. Kern, *Adv. Funct. Mater.* **2002**, *12*, 432–436.
- [32] X. C. Wu, A. M. Bittner, K. Kern, *Langmuir* **2002**, *18*, 4984–4988.
- [33] Relative humidity was found to play an important role in our DPN experiments, since all successful writing experiments were carried out at humidities above 40%. These results support the currently accepted view that relative humidity is essential to the success of DPN. See: S. Rozhok, R. Piner, C. A. Mirkin, *J. Phys. Chem. B* **2003**, *107*, 751–757.
- [34] G. H. Degenhart, B. Dordi, H. Schönherr, G. J. Vancso, *Langmuir* **2004**, *20*, 6216–6224.
- [35] H. Ron, I. Rubinstein, *Langmuir* **1994**, *10*, 4566–4573.
- [36] H. Schmid, B. Michel, *Macromolecules* **2000**, *33*, 3042–3049.
- [37] K. Efimenko, W. E. Wallace, J. Genzer, *J. Colloid Interface Sci.* **2002**, *254*, 306–315.
- [38] M. J. Owen, P. J. Smith, *J. Adhes. Sci. Technol.* **1994**, *8*, 1063–1075.
- [39] S. Perutz, J. Wang, E. J. Kramer, C. K. Ober, K. Elles, *Macromolecules* **1998**, *31*, 4272–4276.
- [40] S. K. Thanawala, M. J. Chaudhury, *Langmuir* **2000**, *16*, 1256–1260.
- [41] a) H. Hillborg, U. W. Gedde, *Polymer* **1998**, *39*, 1991–1998; b) H. Hillborg, J. F. Ankner, U. W. Gedde, G. D. Smith, H. K. Yasuda, K. Wikström, *Polymer* **2000**, *41*, 6851–6863.
- [42] For supramolecular  $\mu\text{CP}$  experiments, the intrinsic hydrophobic character of PDMS ( $\theta_{\text{adv}} = 120^\circ$ ) is insufficient to assure transfer of polar guest molecules from the PDMS stamp onto the  $\beta$ -CD printboard.
- [43] H. Hillborg, N. Tomczak, A. Oláh, H. Schönherr, G. J. Vancso, *Langmuir* **2004**, *20*, 785–794.
- [44] C. Donzel, M. Geissler, A. Bernard, H. Wolf, B. Michel, J. Hilborn, E. Delamarche, *Adv. Mater.* **2001**, *13*, 1164–1167.
- [45] a) B. A. Boukamp, *Solid State Ionics* **1985**, *18–19*, 136–140; b) B. A. Boukamp, *Solid State Ionics* **1986**, *20*, 31–44.

Received: November 11, 2004  
Published online: April 21, 2005